npj | vaccines

Article

Published in partnership with the Sealy Institute for Vaccine Sciences

https://doi.org/10.1038/s41541-026-01439-3

An ESAT-6-convergent prime-boost vaccination combining recombinant BCG expressing *Mycobacterium marinum* ESX-1 and ESAT-6/GLA-SE improves TB protection

Kee Woong Kwon[1,2,7], Hongmin Kim[2,3,7], Hagyu Kim[2,4], Roland Brosch[5] ✉ & Sung Jae Shin[2,3,4,6] ✉

Although Bacille Calmette-Guérin (BCG) protects children against disseminated tuberculosis (TB), its limited efficacy against adult pulmonary TB underscores the need for improved vaccination strategies. We previously developed a recombinant BCG strain expressing the ESX-1 type VII secretion system of *Mycobacterium marinum* (BCG::ESX-1^{Mmar}), which enhances immunogenicity through cytosolic immune signaling while maintaining low virulence. Here, we evaluated an ESAT-6-convergent prime-boost vaccination strategy in which mice were primed with ESX-1-competent BCG::ESX-1^{Mmar} and subsequently boosted with *Mycobacterium tuberculosis* (Mtb)-derived ESAT-6 formulated with the TLR4 agonist adjuvant GLA-SE. Compared with ESAT-6/GLA-SE boosting following parental BCG priming, the BCG::ESX-1^{Mmar}-primed regimen robustly increased antigen-specific CD4$^+$ T cells localized within the lung parenchyma. This strategy markedly enhanced polyfunctional Th1 responses against ESAT-6 and PPD, exceeding those induced by BCG::ESX-1^{Mmar} alone or the conventional BCG-prime/subunit-boost approach. Importantly, ESAT-6 boosting of recombinant BCG::ESX-1^{Mmar} conferred superior long-term protection against hypervirulent Mtb challenge and significantly reduced pulmonary inflammation. Together, these findings demonstrate that leveraging an ESX-1-competent recombinant BCG platform for targeted ESAT-6 boosting can overcome key limitations of classical BCG vaccination and represents a promising strategy for next-generation TB immunization.

Tuberculosis (TB), caused by *Mycobacterium tuberculosis* (Mtb), continues to pose a formidable global health challenge despite decades of control efforts. The 2025 WHO Global Tuberculosis Report highlights that TB has regained its position as the leading cause of death from a single infectious agent, accounting for an estimated 1.23 million deaths in 2024 after being temporarily surpassed by COVID-19 during the pandemic years. Approximately 10 million people develop active TB annually, and nearly one-quarter of the global population carries latent Mtb infection, with the highest burden concentrated in Asia and Africa[1,2]. The COVID-19 pandemic further disrupted diagnostic, treatment, and prevention programs, reversing much of the progress achieved in previous decades[3,4]. Although vaccination remains a key pillar in TB control, the century-old Bacille Calmette-Guérin (BCG) vaccine provides inconsistent and short-lived protection, particularly against adult pulmonary TB with efficacy varying significantly across different geographical regions and populations[5,6], underscoring the

[1]Department of Microbiology, College of Medicine, Gyeongsang National University, Jinju, South Korea. [2]Department of Microbiology, Yonsei University College of Medicine, Seoul, South Korea. [3]Department of Biomedical Sciences, Yonsei University College of Medicine, Seoul, South Korea. [4]Institute for Immunology and Immunological Disease, Yonsei University College of Medicine, Seoul, South Korea. [5]Institut Pasteur, Université Paris Cité, CNRS UMR 6047, Unit for Integrated Mycobacterial Pathogenomics, Paris, France. [6]Department of Microbiology, Graduate School of Medical Science, Brain Korea 21 Project, Yonsei University College of Medicine, Seoul, South Korea. [7]These authors contributed equally: Kee Woong Kwon, Hongmin Kim.
✉e-mail: roland.brosch@pasteur.fr; sjshin@yuhs.ac

urgent need for improved or next-generation vaccines to achieve sustainable global TB elimination.

BCG revaccination was one of the promising strategies given that, if proven to enhance its protective efficacy, this approach could serve as a cost-effective and easily deployable tool to strengthen global TB control efforts. However, the protective effect of BCG revaccination remains limited, with reported efficacy against primary Mtb infection of less than 50%, and notable benefit observed only among adults aged 31–40 years[7]. Ongoing phase 2b clinical trials have yielded inconsistent outcomes, as studies in Malawi and among HIV-negative adolescents failed to demonstrate significantly improved protection[8,9]. In parallel, numerous TB vaccine candidates have been developed through diverse approaches, including live recombinant mycobacterial vaccines and adjuvanted protein subunit formulations, designed either to replace BCG or to enhance BCG-primed immunity[10]. Encouragingly, two live vaccine candidates, VPM1002 and MTBVAC, are currently undergoing multicenter phase 3 clinical trials to evaluate their efficacy based on their safety profile[11,12]. Furthermore, the adjuvanted subunit vaccine M72/AS01$_E$ demonstrated 49.7% efficacy in preventing progression to pulmonary TB for at least 3 years and has advanced to phase 3 clinical evaluation (NCT06062238)[13–15]. Despite these encouraging findings, vaccines with efficacy exceeding 50% are still required to achieve the WHO's End TB strategy targets[16].

Previously, we engineered a low-virulence recombinant BCG vaccine candidate harboring the *esx-1* locus of *Mycobacterium marinum* (BCG::ESX-1^{Mmar}) with improved immunogenic properties regardless of vaccination routes compared to its parental BCG Pasteur 1173P2[17,18]. In mycobacteria, the ESX-1 secretion system constitutes a type VII secretion (T7S) machinery that exports key virulence-associated proteins, thereby mediating host-pathogen interactions through permeabilization of the phagosomal membrane[19]. Incorporation of this functional ESX-1 system into parental BCG resulted in superior protection against Mtb infection, driven by robust activation of innate immunity and potent Th1 responses elicited by ESX-1-secreted effectors[17].

Although the immune correlates of protection against TB remain poorly defined, CD4$^+$ T cells are known to play a central role in host defense against Mtb in animal models[20]. Thus, in the current study, we designed a prime-boost vaccination strategy to efficiently induce antigen (Ag)-specific polyfunctional Th1 responses by leveraging the complementary strengths of two platforms: an improved and more immunogenic recombinant BCG::ESX-1^{Mmar} with a safety profile similar to parental BCG, and ESAT-6 formulated with the TLR4 agonist adjuvant GLA-SE as the booster Ag. The ESAT-6 used for boosting is derived from Mtb and shares approximately 92% overall sequence homology with the ESAT-6 of *Mycobacterium marinum*; notably, the immunodominant CD4$^+$ T cell epitope differs by only a single amino acid between the two proteins[17], supporting functional convergence at the level of Ag-specific T cell recognition. Hereafter, we refer to this strategy as an ESAT-6-convergent prime-boost vaccination. We then evaluated this strategy in the context of infection with the hypervirulent Mtb strain M2, a clinical isolate previously shown to exhibit increased bacterial growth and exacerbated pulmonary pathology compared to laboratory-adapted strains such as H37Rv in mouse models[21]. In this setting parental BCG provides limited protection, whereas our previous work demonstrated enhanced protective efficacy with recombinant BCG::ESX-1^{Mmar}[17]. Here, we sought to determine whether ESAT-6 boosting could further augment the protective capacity of BCG::ESX-1^{Mmar}. Boosting BCG::ESX-1^{Mmar} with ESAT-6 robustly increased localization of Ag-specific T cells within the lung parenchyma and enhanced polyfunctional Th1 responses. Moreover, this regimen conferred superior long-term protection against chronic infection with the hypervirulent Mtb strain M2 compared with either BCG::ESX-1^{Mmar} alone or the parental BCG-primed ESAT-6/GLA-SE-boost strategy. Our results provide a basis for further evaluating ESAT-6-boosted BCG::ESX-1^{Mmar} as a potential approach to enhance the protective efficacy of BCG-based vaccination strategies against TB.

Results

Boosting BCG::ESX-1^{Mmar} with ESAT-6 mediated improved protection against Mtb infection

To investigate the potential of our strategy for exploiting a recombinant BCG-primed subunit boost regimen, BCG::ESX-1^{Mmar}-primed and ESAT-6/GLA-SE intramuscularly boosted mice were challenged with Mtb strain M2 (Fig. 1a). At 6 weeks post-infection, ESAT-6/GLA-SE boosted mice exhibited a significant amelioration of pulmonary inflammation compared with BCG::ESX-1^{Mmar}-only vaccinated mice (Fig. 1b–c). This improvement in lung pathology was accompanied by markedly lower bacterial burdens in both the lungs and spleen, with the boosted group showing superior bacterial control relative to ESAT-6/GLA-SE alone or BCG::ESX-1^{Mmar} alone (Fig. 1d). Together, these findings demonstrate that ESAT-6 boosting can augment recombinant BCG-primed immunity, supporting its potential value as a subunit boost strategy.

ESAT-6/GLA-SE boosting of recombinant BCG::ESX-1^{Mmar} markedly increases Ag-specific CD4$^+$ T cells across both the parenchymal and vascular compartments

Given the enhanced protection observed in our boosting regimen, we next focused our analysis on lung compartments, as mucosal localization of Ag-specific CD4$^+$ T cells within the lung parenchyma has been closely associated with improved pulmonary immunity against Mtb[10,22,23]. Accordingly, we performed a head-to-head comparison of Ag-specific CD4$^+$ T cell responses across the four vaccination groups-parental BCG, BCG plus ESAT-6/GLA-SE, recombinant BCG::ESX-1^{Mmar}, and BCG::ESX-1^{Mmar} plus ESAT-6/GLA-SE (Fig. 2a) to determine how each regimen differentially shaped parenchymal and vascular CD4$^+$ T cell immunity. Using ESAT-6$_{4-17}$:I-A(b) tetramer staining together with intravenous anti-CD45.2 labeling to distinguish vascular (CD45.2$^+$) from parenchymal (CD45.2$^-$) T cells[24], we found that boosting parental BCG with ESAT-6 did not significantly increase ESAT-6-specific CD4$^+$ T cells in either lung compartment compared with BCG alone at 4 weeks after the final immunization. In contrast, BCG::ESX-1^{Mmar} immunization increased the frequency of ESAT-6-specific CD4$^+$ T cells, but only within the lung vasculature whereas ESAT-6 boosting of BCG::ESX-1^{Mmar} elicited markedly higher frequencies of Ag-specific CD4$^+$ T cells in both the lung parenchyma and vasculature compared with the BCG-primed ESAT-6/GLA-SE boost regimen and the BCG::ESX-1^{Mmar}-only group (Fig. 2b–c). Together, these findings indicate that boosting BCG::ESX-1^{Mmar} with ESX-1-secreted Ag ESAT-6 effectively enhances the compartmental abundance of Ag-specific CD4$^+$ T cells.

BCG::ESX-1^{Mmar}-primed mice followed by ESAT-6/GLA-SE vaccination exhibited enhanced capacity of eliciting Ag-specific CD4$^+$ Th1 responses

Based on observations, we further examined the magnitude and quality of polyfunctional Ag-specific T cells (following the gating strategy outlined in Supplementary Fig.1), given that robust Th1-type cellular immunity directed against mycobacterial Ags is a key determinant of protection against TB[25]. To assess the production of IFN-γ, TNF, and IL-2 by Ag-specific CD4$^+$ T cells, lymphocytes were isolated from the lungs and spleen 4 weeks after the final immunization. Prior to tissue collection, mice received an intravenous anti-CD45.2 injection, and the isolated cells were then stimulated with ESAT-6 or PPD for intracellular cytokine staining. The number of PPD-specific IFN-γ$^+$, TNF$^+$, and IL-2$^+$ CD4$^+$ T cells in the lung parenchyma was higher in the BCG::ESX-1^{Mmar}-primed ESAT-6/GLA-SE boosted group than in either the BCG-primed ESAT-6/GLA-SE boosted group or the BCG::ESX-1^{Mmar}-only group (Fig. 3a–b). In addition, the BCG::ESX-1^{Mmar}-primed ESAT-6/GLA-SE boost regimen markedly enhanced the polyfunctionality of Ag-specific CD4$^+$ T cells, characterized by the co-production of IFN-γ, TNF, and/or IL-2 within the lung parenchyma (Fig. 3c; Supplementary Fig. 2a). When stimulated with ESAT-6, the BCG-primed ESAT-6/GLA-SE boosted group also exhibited increased numbers of ESAT-6-specific CD4$^+$ T cells compared with BCG alone; however, these increases were further augmented in the BCG::ESX-1^{Mmar}-primed ESAT-6/GLA-SE boosted group, which displayed

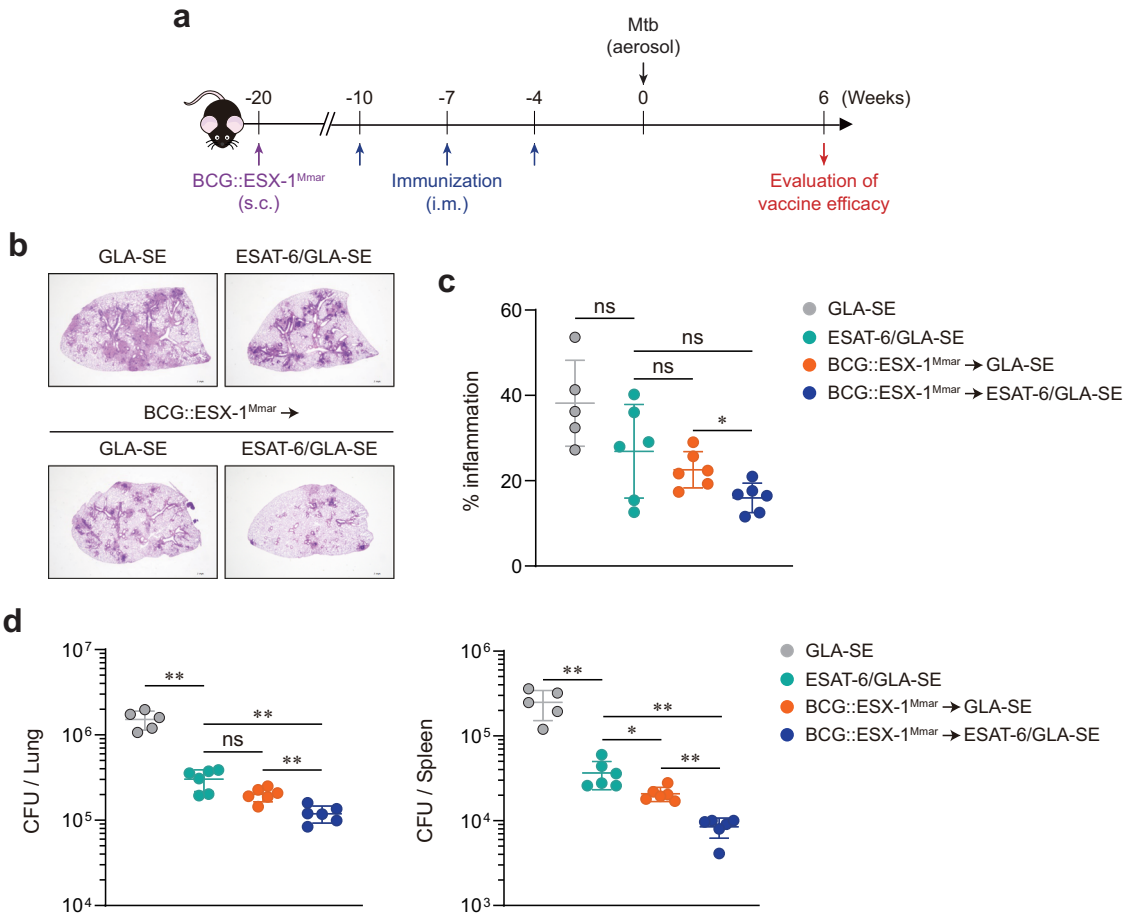

Fig. 1 | Evaluation of vaccine efficacy in BCG::ESX-1^{Mmar}-primed ESAT-6/GLA-SE boosted mice following infection with Mtb M2. a Experimental design. Mice (n = 5–6 per group) were immunized with BCG::ESX-1^{Mmar} and, 10 weeks later, received three intramuscular doses of ESAT-6/GLA-SE (blue arrows) prior to aerosol infection with Mtb M2 (black arrow). Bacterial burden and lung pathology were assessed 6 weeks after infection (red arrow). **b** Representative H&E-stained lung sections from each group (10×, scale bars = 2.0 mm). **c** Quantification of inflamed areas in the superior lobe of the right lung. **d** Bacterial loads in lungs and spleens at 6 weeks post-infection. Data are presented as mean ± SD and are representative of at least two independent experiments. Statistical comparisons were performed using the Mann–Whitney U test. n.s., not significant, $^{*}p < 0.05$, and $^{**}p < 0.01$.

the highest numbers of ESAT-6-specific CD4^{+} T cells among all groups (Fig. 3a, d). Consistent with this pattern, ESAT-6-specific polyfunctional CD4^{+} T cells were most abundant in the BCG::ESX-1^{Mmar}-primed ESAT-6/GLA-SE boosted group, exceeding the levels observed in both the BCG-primed ESAT-6/GLA-SE boosted and the BCG::ESX-1^{Mmar}-only groups (Fig. 3e; Supplementary Fig. 2b). In the lung vasculature, comparable patterns were observed, with the BCG::ESX-1^{Mmar}-primed ESAT-6/GLA-SE boosted group again showing the highest numbers of PPD- and ESAT-6-specific CD4^{+} T cells and the greatest frequencies of polyfunctional subsets across all vaccination groups (Fig. 4a–d; Supplementary Fig. 3). Similar trends extended to systemic immunity, as splenic analyses revealed the same hierarchy of Ag-specific CD4^{+} T cell numbers and polyfunctionality, with the BCG::ESX-1^{Mmar}-primed ESAT-6/GLA-SE boosted regimen consistently outperforming all other groups (Supplementary Fig. 4). Together, these findings show that ESAT-6 boosting of BCG::ESX-1^{Mmar} consistently amplifies both the magnitude and polyfunctional quality of Ag-specific CD4^{+} T cells across pulmonary and systemic compartments.

ESAT-6 subunit boosting improves the protective efficacy of BCG::ESX-1^{Mmar} against hypervirulent Mtb M2 infection

At 12 weeks post-Mtb infection, pulmonary inflammation differed markedly among the vaccinated groups. Consistent with our previous studies using the hypervirulent Mtb M2 strain[2,17], vaccination with recombinant BCG::ESX-1^{Mmar} again produced a clear reduction in lung inflammation relative to the vaccination with parental BCG. Boosting parental BCG with ESAT-6 formulated in GLA-SE did not improve its inflammatory outcome compared with parental BCG alone, mirroring our earlier observation[2]. In contrast, ESAT-6 boosting further enhanced the protective effect of recombinant BCG::ESX-1^{Mmar}, resulting in the lowest pulmonary inflammatory burden among all vaccinated groups (Fig. 5a–b). The same hierarchy was reflected in bacterial burden measurements. ESAT-6/GLA-SE boosting did not enhance the performance of parental BCG, as pulmonary and splenic CFU levels remained comparable between the BCG-alone and BCG-primed ESAT-6/GLA-SE boosted groups. In contrast, recombinant BCG::ESX-1^{Mmar} again reduced CFU more effectively than parental BCG, and this effect became more pronounced when recombinant BCG::ESX-1^{Mmar} was boosted with ESAT-6/GLA-SE (Fig. 5c). To determine whether the protective efficacy of this regimen extended beyond the peak effector phase, in a pilot experiment we increased the interval between the final ESAT-6 boost and Mtb challenge from the previously used 4 weeks to 8 weeks (Supplementary Fig. 5a). Prior to Mtb infection, ESAT-6-boosted BCG::ESX-1^{Mmar} mice displayed higher frequencies and greater polyfunctionality of Ag-specific CD4^{+} T cells compared with other vaccination groups, indicating preserved functional responsiveness even after the prolonged interval between the final booster and Mtb challenge (Supplementary Fig. 5b and c). Under this delayed challenge setting, ESAT-6 boosting of

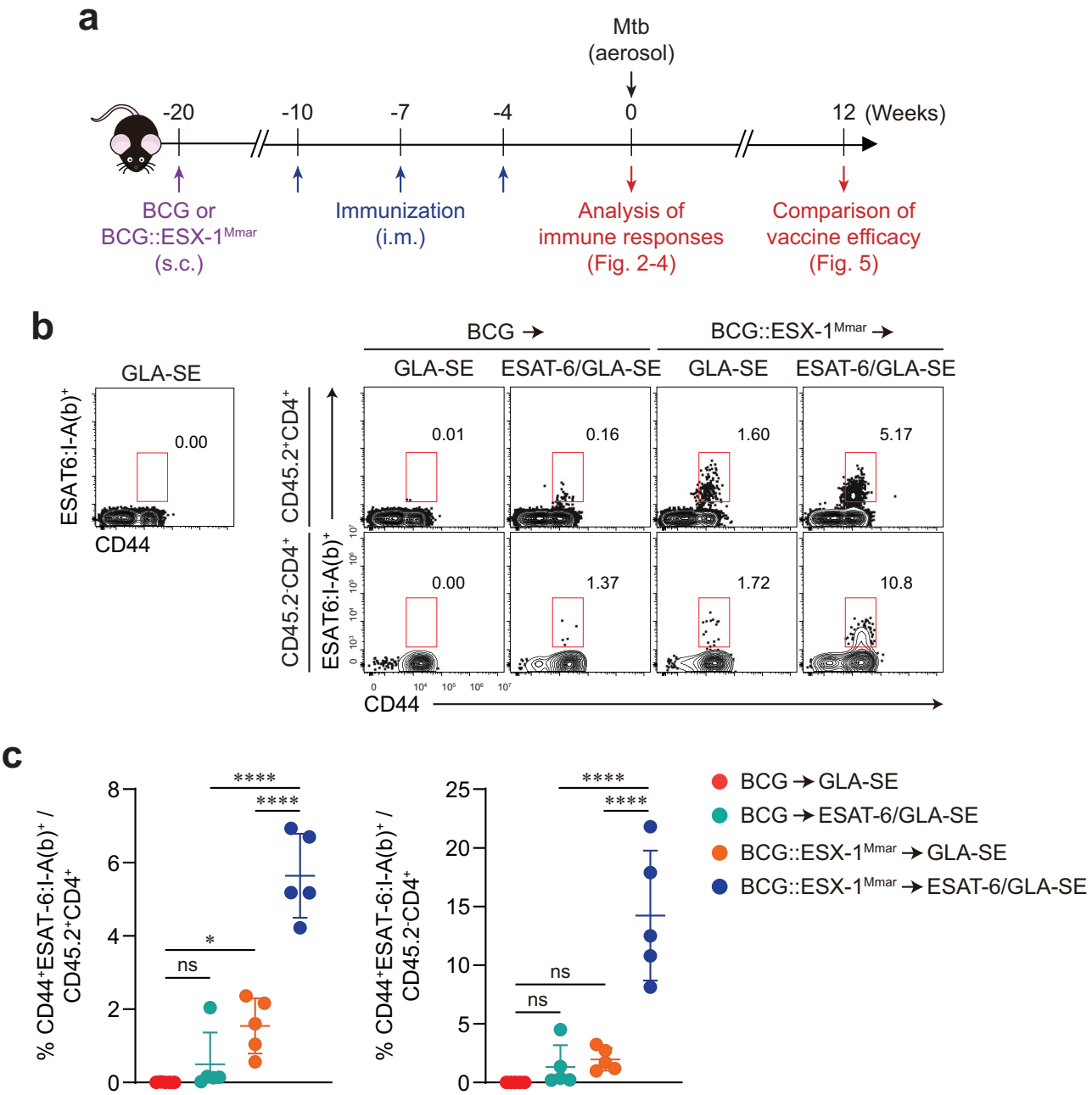

Fig. 2 | Analysis of antigen-specific CD4$^+$ T cells in lung parenchymal and vascular compartments following vaccination. a Experimental scheme. Mice were immunized with parental BCG or recombinant BCG::ESX-1^{Mmar} and, 10 weeks later, received three intramuscular doses of ESAT-6/GLA-SE (blue arrows) prior to aerosol challenge with Mtb M2 (black arrow). Lung immunological analyses were performed 4 weeks after the final immunization, before Mtb infection (red arrow). Bacterial burden and histopathology were assessed at 12 weeks post-infection (red arrow). **b** Representative flow cytometry plots showing ESAT-6_{4-17}:I-A(b)$^+$ CD4$^+$ T cells in lung parenchymal (CD45.2$^-$) and intravascular (CD45.2$^+$) compartments ($n = 5$). Numbers indicate the frequency of Ag-specific CD4$^+$ T cells within each compartment. **c** Summary of Ag-specific CD4$^+$ T cell frequencies in lung parenchyma and vasculature. Data represent mean ± SD and are representative of at least two independent experiments. Statistical analyses were performed using one-way ANOVA with Tukey's *post hoc* test. n.s., not significant, $^*p < 0.05$, and $^{****}p < 0.0001$. Note that the experimental scheme shown in panel a illustrates the entire timeline of the study. Panels **b** and **c** of Fig. 2 and panels **a**–**e** of Figs. 3 and 4 present immunological analyses performed 4 weeks after the 3rd booster immunization, corresponding to the time point at which the remaining mice were challenged with Mtb. Protection data, including bacterial burden measured 12 weeks after challenge, are shown in Fig. 5.

BCG::ESX-1^{Mmar} remained associated with significantly reduced pulmonary bacterial burden at 4 weeks post challenge as compared with the other vaccination groups, thereby suggesting that the enhanced protection was maintained beyond the immediate post-vaccination period (Supplementary Fig. 5d). Together, these findings support the potential of ESAT-6/GLA-SE boosting to further enhance the protective efficacy of recombinant BCG::ESX-1^{Mmar}, highlighting this prime-boost strategy as a promising approach to strengthen BCG-based vaccination against TB.

Discussion

Despite a century of global use, the BCG vaccine provides incomplete and variable protection against pulmonary TB, particularly in adolescents and adults. Recent clinical data have highlighted the limitations of BCG revaccination, which shows inconsistent and age-restricted efficacy[7,8]. These shortcomings underscore the need for improved BCG-based boosting strategies capable of overcoming the immunological constraints of the classical platform. In this context, our study demonstrates that a prime-

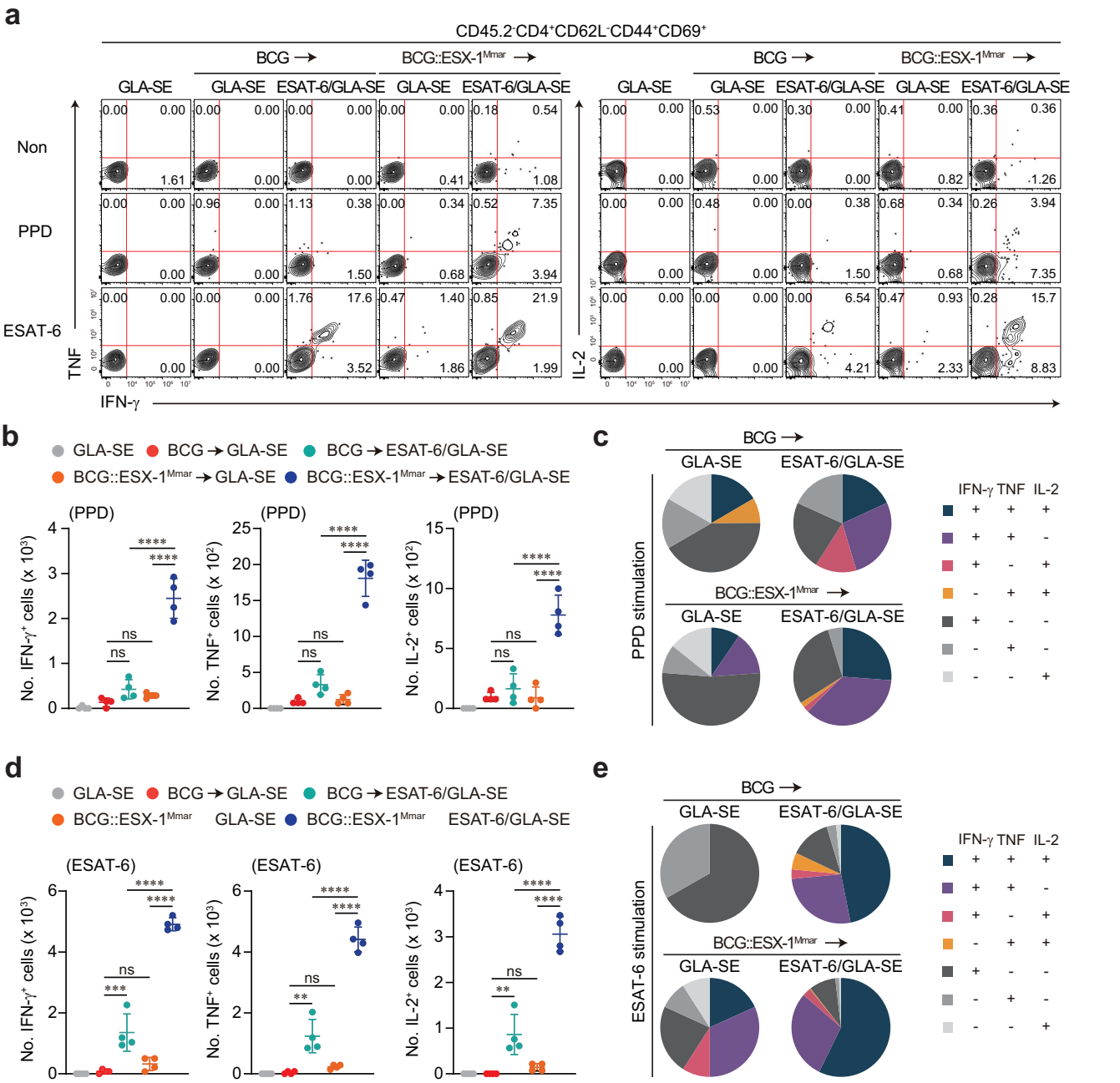

Fig. 3 | Analysis of CD4⁺ T cell responses in the lung parenchyma of mice following BCG- or BCG::ESX-1^{Mmar}-primed ESAT-6/GLA-SE vaccination 4 weeks after the 3rd booster administration. a Representative flow cytometry plots showing IFN-γ⁺, TNF⁺, or IL-2⁺ CD4⁺ T cells in the lung parenchyma. The numbers in plots indicate the IFN-γ⁺TNF⁺, IFN-γ⁺TNF⁻, and IFN-γ⁻TNF⁺ / IFN-γ⁺IL-2⁺, IFN-γ⁺IL-2⁻, and IFN-γ⁻IL-2⁺. **b** Quantification of PPD-stimulated IFN-γ⁺, TNF⁺, or IL-2⁺ CD4⁺ T cells in the lung parenchyma ($n = 4$). **c** Polyfunctionality profiles of PPD-stimulated CD4⁺CD44⁺CD62L⁻CD69⁺ T cells, shown as pie charts representing the proportions of triple-, double-, and single-cytokine–producing subsets. **d** Quantification of ESAT-6–stimulated IFN-γ⁺, TNF⁺, or IL-2⁺ CD4⁺ T cells in the lung parenchyma ($n = 4$). **e** Polyfunctionality profiles of ESAT-6–stimulated CD4⁺CD44⁺CD62L⁻CD69⁺ T cells, represented as pie charts showing the distribution of triple-, double-, and single-cytokine–producing populations. Data represent mean ± SD and are representative of at least two independent experiments. Statistical analyses were performed using one-way ANOVA with Tukey's *post hoc* test. n.s., not significant, $^{**}p < 0.01$, $^{***}p < 0.001$, and $^{****}p < 0.0001$.

boost regimen combining BCG::ESX-1^{Mmar} with an ESAT-6/GLA-SE enhances both immunogenicity and protection against chronic infection with the hypervirulent Mtb strain M2.

In line with our previous work[17], the recombinant BCG strain conferred measurable protection at 6 weeks post-infection, and this effect was further strengthened by ESAT-6 boosting. A head-to-head comparison revealed that the immunological consequences of boosting were strongly influenced by the priming platform. While boosting parental BCG exerted minimal effects on T cell distribution, priming with BCG::ESX-1^{Mmar} established an immunological environment that promoted the selective accumulation of Ag-specific CD4⁺ T cells within the lung parenchyma. This quantitative and qualitative shift suggests that ESX-1 competence is an important determinant for directing subunit-boosted immunity toward pulmonary compartments critical for protection.

In the broader context of TB vaccine development, booster strategies employing subunit vaccine candidates have frequently been pursued to broaden antigenic coverage and reinforce BCG-primed immunity as vaccine-induced protection wanes[16]. Indeed, several subunit vaccines have

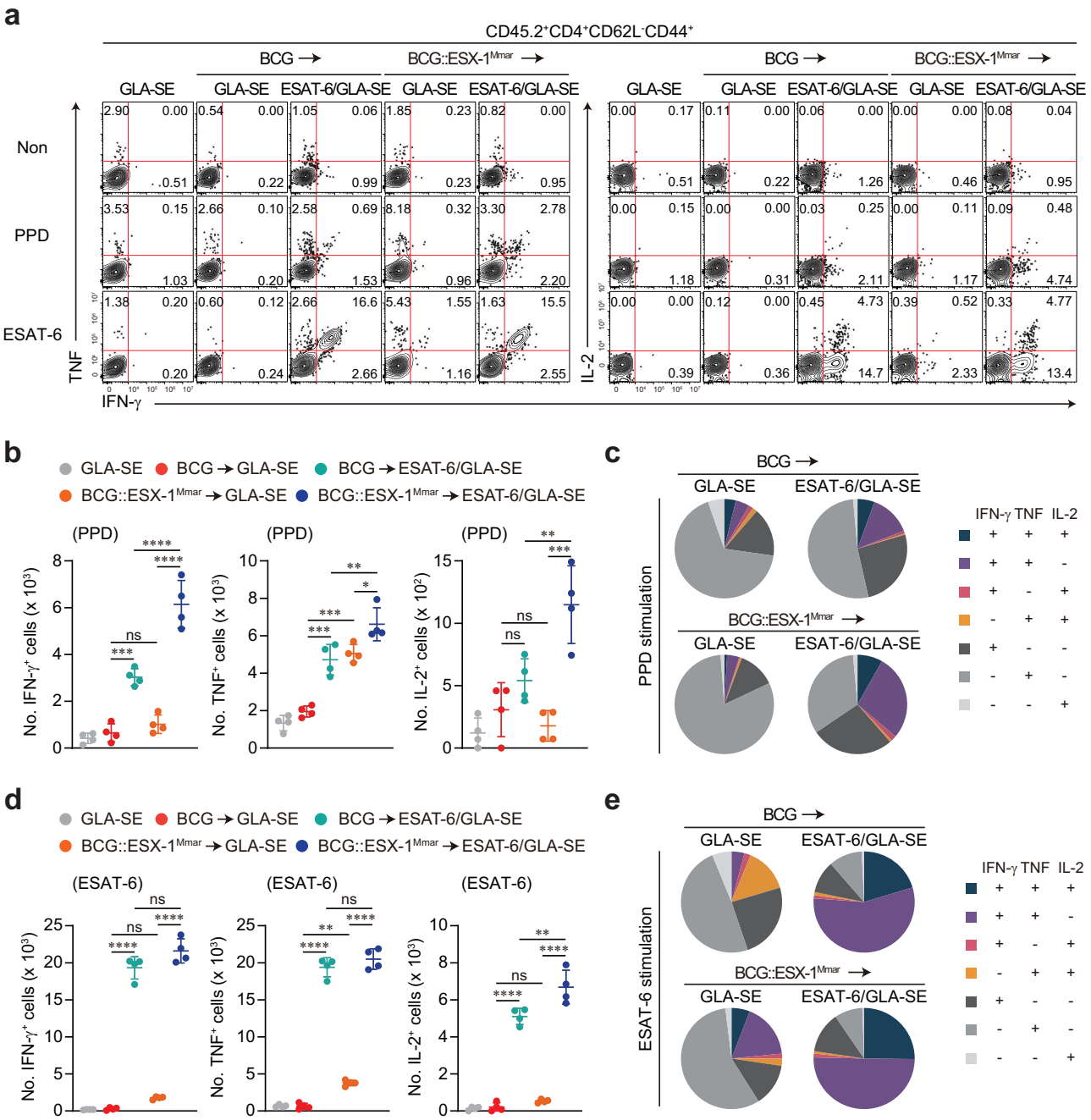

Fig. 4 | Analysis of CD4⁺ T cell responses in the lung vasculature of mice following BCG- or BCG::ESX-1^{Mmar}-primed ESAT-6/GLA-SE vaccination 4 weeks after 3rd booster administration. a Representative flow cytometry plots showing IFN-γ⁺, TNF⁺, or IL-2⁺ CD4⁺ T cells in the lung vasculature. The numbers in plots indicate the IFN-γ⁺TNF⁺, IFN-γ⁺TNF⁻, and IFN-γ⁻TNF⁺ / IFN-γ⁺IL-2⁺, IFN-γ⁺IL-2⁻, and IFN-γ⁻IL-2⁺. **b** Quantification of PPD-stimulated IFN-γ⁺, TNF⁺, or IL-2⁺ CD4⁺ T cells in the lung vasculature ($n = 4$). **c** Polyfunctionality profiles of PPD-stimulated CD4⁺CD44⁺CD62L⁻CD69⁺ T cells, shown as pie charts representing the proportions of triple-, double-, and single-cytokine–producing subsets. **d** Quantification of ESAT-6–stimulated IFN-γ⁺, TNF⁺, or IL-2⁺ CD4⁺ T cells in the lung vasculature ($n = 4$). **e** Polyfunctionality profiles of ESAT-6–stimulated CD4⁺CD44⁺CD62L⁻CD69⁺ T cells, represented as pie charts showing the distribution of triple-, double-, and single-cytokine–producing populations. Data represent mean ± SD and are representative of at least two independent experiments. Statistical analyses were performed using one-way ANOVA with Tukey's *post hoc* test. n.s., not significant, $*p < 0.05$, $**p < 0.01$, $***p < 0.001$, and $****p < 0.0001$.

elicited enhanced booster-induced and/or de novo CD4⁺ T cell responses when administered following BCG priming, accompanied by improved protective efficacy[13,26–28]. However, accumulating evidence suggests that the effectiveness of boosting may be shaped by the immunological context established during the priming phase[29]. A critical component of this context is the primary activation of Ag-specific CD4⁺ T helper cells, which can influence the magnitude, functional quality, and durability of vaccine-induced immune responses[30]. Accordingly, the CD4⁺ T cell priming properties of diverse adjuvants[31,32], immunization routes[33,34], and delivery systems-including live recombinant mycobacterial platforms such as recombinant BCG[17,35]-have been characterized to facilitate the rational design of effective prime-boost vaccination strategies.

Within this framework, our findings indicate that ESAT-6 boosting elicits distinct immunological outcomes depending on the priming platform. While ESAT-6/GLA-SE boosting following parental BCG had minimal impact on pulmonary T cell localization or functional quality,

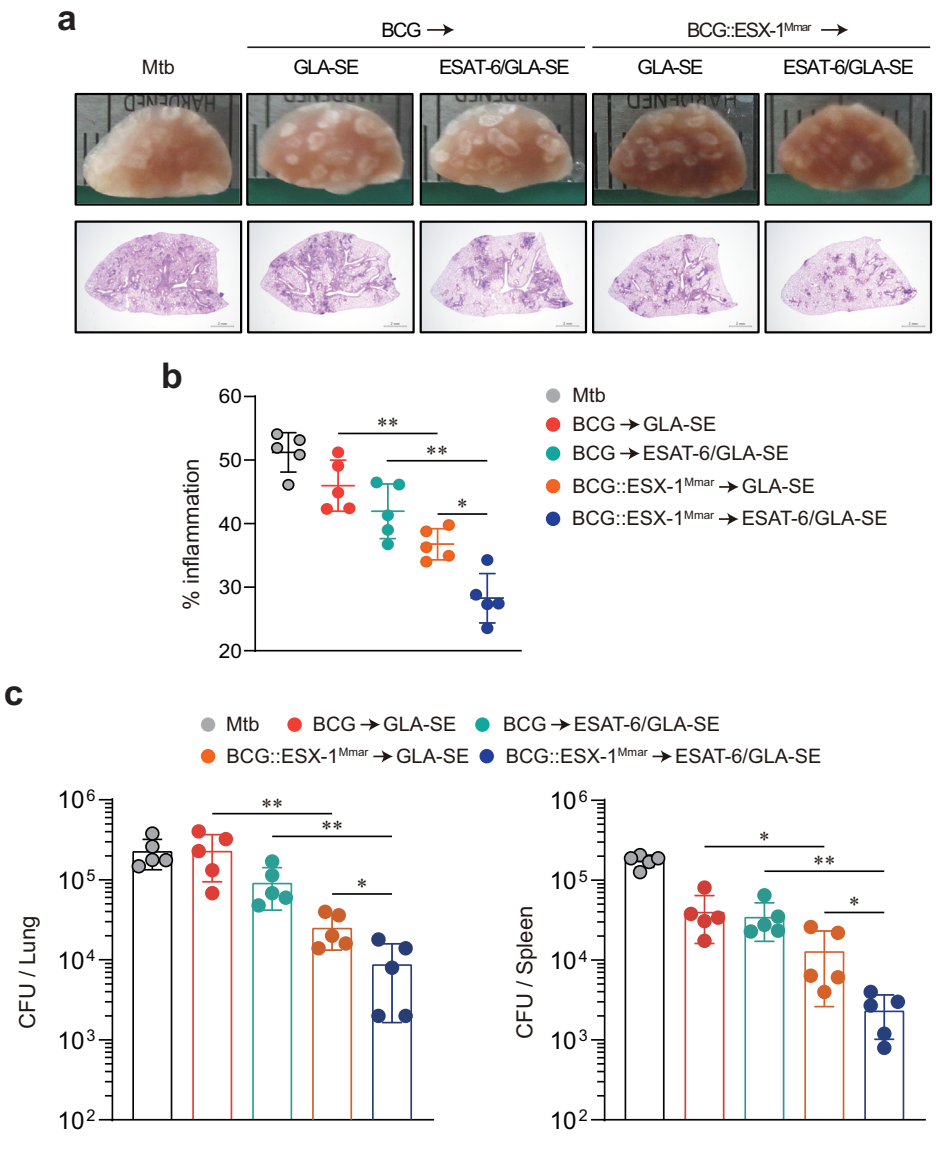

Fig. 5 | ESAT-6/GLA-SE boosting enhances the long-term protective efficacy of recombinant BCG::ESX-1^{Mmar} against hypervirulent Mtb M2 infection. a Gross pathology and H&E staining of lungs of each group at 12 weeks after aerosol infection with Mtb M2 (10×, scale bars = 2.0 mm). **b** Quantification of lung inflammation based on the inflamed area of the superior lobe of the right lung. **c** Bacterial loads in the lungs and spleens of each group at 12 weeks post-infection. Data are presented as mean ± SD and are representative of at least two independent experiments. Statistical comparisons were performed using the Mann–Whitney U test. n.s., not significant, $^{*}p < 0.05$, and $^{**}p < 0.01$.

administration of the same booster after priming with BCG::ESX-1^{Mmar} markedly enhanced Ag-specific CD4^{+} T cell responses. These results suggest that the benefit of boosting is closely linked to the immunological context established during priming, and that prime-boost strategies may be particularly effective when the priming platform engages cytosolic sensing pathways and promotes Th1 polarization through ESX-1-dependent mechanisms[17,19].

The superior efficacy of this regimen can therefore be attributed to the enhanced priming quality of the recombinant BCG platform. Unlike parental BCG, which lacks a functional ESX-1 system due to the deletion of the RD1 region, BCG::ESX-1^{Mmar} restores the functions of the ESX-1-mediated Ag secretion and cytosolic access, facilitating early priming of ESAT-6-specific T cells and activation of innate sensing pathways such as cGAS–STING[36]. Consequently, ESAT-6/GLA-SE boosting likely functions predominantly as an anamnestic stimulus that expands pre-existing, functionally competent memory T cells rather than initiating a de novo primary response[17,22]. The resulting enrichment of polyfunctional Th1 cells within the lung parenchyma is particularly relevant, as parenchymal rather than intravascular T cells are required for direct interaction with infected macrophages and effective restriction of Mtb replication[22,23,25]. Together, our results demonstrate that restoring ESX-1 functionality-even using a safer *M. marinum*-derived system-fundamentally improves the localization of Ag-specific T cells in the lung parenchyma and functional competence of the cellular immune response against hypervirulent Mtb[19].

Several limitations of this study warrant further discussion. First, while our regimen significantly boosted immunity, we did not perform a detailed phenotypic analysis of ESAT-6-specific T cells with respect to terminal differentiation markers such as KLRG1 or PD-1. Given that persistent exposure to ESAT-6 can drive T cell dysfunction or exhaustion[10,37], verifying the memory transition and differentiation state is crucial, as avoiding terminal differentiation is essential for sustained parenchymal migration and long-term protection[38]. Second, although we observed a correlation between parenchymal T cell accumulation and protection, we did not directly demonstrate the requirement of these cells using pharmacological inhibitors. Future studies employing FTY720 to block the recruitment of newly activated T cells from lymphoid organs would be valuable to confirm whether the pre-existing parenchymal T cell pool is the primary determining factor for the observed protective capacity[22]. Third, while our current study focused primarily on ESAT-6, other ESX-1-associated effectors-such as CFP-10 or the PE/PPE family proteins-might also significantly contribute to the overall protective immunity[39,40]. Future investigations into whether co-immunization with a broader repertoire of ESX-1-secreted antigens could further synergize with our recombinant BCG platform

would be of great interest, potentially leading to even more robust and comprehensive protection against diverse Mtb strains. Fourth, our study was conducted exclusively in female mice. Biological sex is increasingly recognized as an important determinant of vaccine-induced immunity, including in the context of TB vaccination[41]. Therefore, future studies incorporating both male and female models will be necessary to determine whether the enhanced priming and boosting effects observed with BCG::ESX-1^{Mmar} are broadly applicable. Lastly, it is crucial to acknowledge that the immense diversity in phenotypic, genotypic, and pathogenic traits among various Mtb lineages can significantly alter vaccine performance[42,43]. Therefore, these strain-specific differences must be integrated into any comprehensive evaluation of protective efficacy. Furthermore, the durability of vaccine-induced responses is a critical concern. In healthy children, the capacity of central memory T cells to proliferate and differentiate into active effector T cells upon BCG stimulation has been shown to decline progressively with age[27,44]. This waning of cellular immunity suggests that the protection established by neonatal BCG is not lifelong, emphasizing that booster vaccinations are essential to sustain Ag-specific T cell populations and prolong the period of protection. In this regard, the results of a pilot experiment using a delayed challenge model suggests that enhanced protection following ESAT-6 boosting of recombinant BCG can still be observed when the interval between the final immunization and infection was extended. This effect was seen, together with maintained multifunctional Ag-specific CD4$^+$ T cell responses prior to challenge. Nevertheless, future studies with extended intervals and comprehensive memory phenotyping will be needed to confirm the long-term durability of this vaccination strategy.

In summary, our study exemplifies a synergistic prime-boost strategy that significantly enhances protection against hypervirulent Mtb. By combining the improved priming capacity of recombinant BCG::ESX-1^{Mmar} with a targeted ESAT-6 boost, we achieved superior control of bacterial burden and lung inflammation through the robust recruitment of polyfunctional CD4$^+$ T cells into the lung parenchyma. These findings suggest that leveraging the ESX-1 secretion system can overcome the limitations of the classical BCG platform. To advance these findings from the preclinical stage to clinical application, further mechanistic studies across diverse animal models will be essential to ensure the safety and sustained efficacy of this next-generation vaccination strategy.

Methods

Ethics statement

All animal studies were performed in accordance with Korean Food and Drug Administration (KFDA) guidelines. The experimental protocols used in this study were reviewed and approved by the Ethics Committee and Institutional Animal Care and Use Committee (Permit Number: 2021-0279) of the Laboratory Animal Research Center at Yonsei University College of Medicine (Seoul, Korea).

Animals

Six- to seven-week-old specific pathogen-free female C57BL/6 J mice were purchased from Japan SLC, Inc. (Shizuoka, Japan). Mice were maintained under barrier conditions in the ABSL-3 facility at the Yonsei University College of Medicine. All mice were housed in a constant temperature/humidity environment (24 ± 1 °C, 50 ± 5%) under light-controlled conditions (12 h light-dark cycle; 7 am on and 7 pm off) and fed a sterile commercial mouse diet with ad libitum access to water.

Expression and purification of recombinant proteins

The *esat-6* was amplified from Mtb H37Rv ATCC27294 genomic DNA using following primer sets: *esat-6* forward, 5'-AAGCTTATGACAGAGCAGCAGTGGAAT-3' (*HindIII*), and reverse, 5'-CTCGAGTGCGAACATCCCAGTGACGTT-3' (*XhoI*). The DNA fragments of ESAT-6 was cloned into the restriction sites (ESAT-6; *HindIII* and *Xho I*) of the plasmid pET22b (+) vector (Novagen, Madison, WI, USA), and the c-terminal His-tag present in the plasmid was included. The product was transformed into *Escherichia coli* BL21, which was induced to express proteins by isopropyl β-D-1-thiogalactopyranoside (IPTG). IPTG was added at a final concentration of 1 mM. The recombinant ESAT-6 was prepared as described previously[10]. All the uncropped and unprocessed gel images are provided in the Supplementary Fig. 6.

Preparation of mycobacteria strains

Mycobacterial strains included Mtb M2 (ITRC, Changwon, Gyeongsangnam-do, South Korea) and BCG (Pasteur strain 1173P2; Pasteur Institute, Paris, France). Recombinant strain BCG::ESX-1^{Mmar} was generated and cultivated as described previously[17]. All mycobacteria used in this study were prepared as described previously[2,17,45].

Immunization and challenge protocol

For all in vivo experiments BCG or BCG::ESX-1^{Mmar} was subcutaneously administered once with 1.0×10^6 CFUs, then mice were immunized with 1 μg of ESAT-6 formulated in GLA-SE 10 weeks after priming with BCG or BCG::ESX-1^{Mmar}. The ESAT-6/GLA-SE boost was given as an intramuscular injection three times at 3 weeks intervals. Four weeks after the final boost, immunized mice were aerogenically challenged with the Mtb M2 strain as previously described[2]. In an independent pilot experiment, the interval between the final ESAT-6 boost and Mtb challenge was extended to 8 weeks to evaluate the durability of vaccine-induced immunogenicity and protection. Aerosol infection was performed using a Glas-Col aerosol apparatus (Terre Haute, IN, USA) adjusted to achieve an initial infectious dose of 200 CFUs. At 12 weeks post-challenge, mice from each group were euthanized in a euthanasia chamber following the gradual carbon dioxide (CO_2) filling method from a compressed CO_2 gas cylinder followed by KFDA guidelines for subsequent analysis.

In vivo intravascular labeling

For intravenous staining, mice were injected intravenously with FITC-conjugated anti-CD45.2 (104; BD Biosciences) as previously described[10]. Briefly, 4 μg/mouse of antibody was administrated in a total volume of 200 μl. Three minutes after antibody injection, mice were euthanized as described above, and single cell suspensions were prepared as described below.

Tetramer, surface and intracellular cytokine staining

Tetramer (ESAT-6_{4-17}:I-A(b)) conjugated to PE and corresponding negative controls (hCLIP:I-A(b)) were provided by the NIH tetramer facility (Atlanta, USA). Single cell suspensions of the lungs and spleens were prepared as previously described[46]. Single cell suspensions of each group were stained with MHC-II tetramers for 30 min at 37 °C. Then, single cell suspensions were first washed with 2% FBS containing PBS and blocked with anti-CD16/32 (BD Biosciences) at 4 °C for 20 min. For phenotypic analysis, single cell suspensions were stained with the following antibodies for 20 min at 4 °C; ThermoFisher Scientific (Waltham, MA, USA): Live/Dead Fixable Viability Dye eFluor 780; Biolegend (San Diego, CA, USA): CD4 (RM4-5)-PerCP-Cy5.5, CD8 (53-6.7)-BV785, CD62L (MEL-14)-Alexa700, CD44 (IM7)-BV421, and CD69 (H1.2F3)-PE/Dazzle 594. For intracellular staining, cells were fixed, permeabilized, and stained intracellularly with following antibodies; BD Biosciences: IFN-γ (XMG1.2)-PE, IL-2 (JES6-5H4)-PE-Cy7, and TNF (MP6-XT22)-APC. To detect intracellular cytokines in T cells from the lungs and spleens, single cell suspensions (1×10^6 cells) from infected or immunized mice were stimulated with ESAT-6 (1 μg/ml) or PPD (Purified Protein Derivative; 5 μg/ml) at 37 °C for 9 h in the presence of GolgiPlug and GolgiStop (BD Biosciences). PPD was kindly provided by Dr. Michael Brennan at Aeras (Rockville, MD, USA). Then, cells were analyzed using the CytoFLEX S flow cytometer (Beckman Coulter, Indianapolis, IN, USA), and subsequent analysis was performed using FlowJo version 10 software (TreeStar, Ashland, OR, USA).

Bacterial enumeration and assessment of pulmonary inflammation

To enumerate the number of bacteria, mice were euthanized with CO_2, and lungs and spleens were homogenized. The number of viable bacteria was determined by plating serial dilutions of the organ homogenates onto Middlebrook 7H10 agar (Difco, Detroit, MI, USA) supplemented with 10% OADC (Difco) and amphotericin B (Sigma Aldrich, USA). Colonies were counted after 4 weeks of incubation at 37 °C. For histopathological analysis, the middle cross-section from entire superior lobes of the right lung were stained with hematoxylin and eosin (H&E) and assessed for the severity of inflammation. The level of inflammation in the lungs was evaluated by ImageJ (National Institutes of Health, USA) program, as previously described[47].

Statistical analysis

Data for all experiments are presented as the mean ± SD. For immunological analysis, the significance of differences between samples was assessed by one-way ANOVA after Tukey's post-test for multiple comparisons. For CFU and histopathology analysis, Mann–Whitney rank test was used when comparing the differences between two different groups. For statistical analysis, GraphPad Prism version 8.00 for Windows was used (GraphPad Software, La Jolla California USA, www.graphpad.com). Differences having $^{*}p < 0.05$, $^{**}p < 0.01$, $^{***}p < 0.001$, or $^{****}p < 0.0001$ were considered statistically significant.

Data availability

All data upon which conclusions are drawn are included in the manuscript or in the supplemental information file provided.

Received: 30 December 2025; Accepted: 29 March 2026;
Published online: 10 April 2026

References

1. World Health Organization. Global Tuberculosis Report https://iris.who.int/server/api/core/bitstreams/e97dd6f4-b567-4396-8680-717bac6869a9/content (2025).
2. Kwon, K. W. et al. BCG-booster vaccination with HSP90-ESAT-6-HspX-RipA multivalent subunit vaccine confers durable protection against hypervirulent Mtb in mice. *NPJ Vaccines* **9**, 55 (2024).
3. Pai, M., Kasaeva, T. & Swaminathan, S. Covid-19's devastating effect on tuberculosis care - a path to recovery. *N. Engl. J. Med* **386**, 1490–1493 (2022).
4. Hogan, A. B. et al. Potential impact of the COVID-19 pandemic on HIV, tuberculosis, and malaria in low-income and middle-income countries: a modelling study. *Lancet Glob. Health* **8**, e1132–e1141 (2020).
5. Lange, C. et al. 100 years of *Mycobacterium bovis* bacille Calmette-Guérin. *Lancet Infect. Dis.* **22**, e2–e12 (2022).
6. Nemes, E. et al. Prevention of *M. tuberculosis* Infection with H4:IC31 Vaccine or BCG Revaccination. *N. Engl. J. Med* **379**, 138–149 (2018).
7. Shaji, A., Verma, A., Bhaskar, A. & Dwivedi, V. P. BCG and beyond: unlocking new frontiers in TB vaccine development. *Front Immunol.* **16**, 1608104 (2025).
8. Glynn, J. R. et al. BCG re-vaccination in Malawi: 30-year follow-up of a large, randomised, double-blind, placebo-controlled trial. *Lancet Glob. Health* **9**, e1451–e1459 (2021).
9. Schmidt, A. C. et al. BCG revaccination for the prevention of *Mycobacterium tuberculosis* infection. *N. Engl. J. Med* **392**, 1789–1800 (2025).
10. Kwon, K. W. et al. Adjunctive beneficial effect of c-di-GMP, a STING agonist, in enhancing protective efficacy of TLR4-adjuvanted tuberculosis subunit vaccine formulations. *J. Biomed. Sci.* **32**, 52 (2025).
11. Tameris, M. et al. Safety, reactogenicity, and immunogenicity of MTBVAC in infants: a phase 2a randomised, double-blind, dose-defining trial in a TB endemic setting. *EBioMedicine* **114**, 105628 (2025).
12. Cotton, M. F. et al. Safety and immunogenicity of VPM1002 versus BCG in South African newborn babies: a randomised, phase 2 non-inferiority double-blind controlled trial. *Lancet Infect. Dis.* **22**, 1472–1483 (2022).
13. Tait, D. R. et al. Final analysis of a trial of M72/AS01(E) vaccine to prevent tuberculosis. *N. Engl. J. Med* **381**, 2429–2439 (2019).
14. Tozer, L. Promising tuberculosis vaccine gets US$550-million shot in the arm. *Nature* https://doi.org/10.1038/d41586-023-02171-x (2023).
15. Gates, Wellcome rekindle TB vaccine. *Nat. Biotechnol.* **41**, 1039 (2023).
16. Woodworth, J. S. et al. A *Mycobacterium tuberculosis*-specific subunit vaccine that provides synergistic immunity upon co-administration with Bacillus Calmette-Guérin. *Nat. Commun.* **12**, 6658 (2021).
17. Gröschel, M. I. et al. Recombinant BCG expressing ESX-1 of *Mycobacterium marinum* combines low virulence with cytosolic immune signaling and improved TB protection. *Cell Rep.* **18**, 2752–2765 (2017).
18. Sayes, F. et al. Improved immune responses and tuberculosis protection by aerosol vaccination with recombinant BCG expressing ESX-1 from *Mycobacterium marinum*. *PLoS Pathog.* **22**, e1013992 (2026).
19. Gröschel, M. I. et al. ESX secretion systems: mycobacterial evolution to counter host immunity. *Nat. Rev. Microbiol.* **14**, 677–691 (2016).
20. Sathkumara, H. D. et al. Mucosal delivery of ESX-1-expressing BCG strains provides superior immunity against tuberculosis in murine type 2 diabetes. *Proc. Natl. Acad. Sci. USA* **117**, 20848–20859 (2020).
21. Kang, T. G. et al. Viral coinfection promotes tuberculosis immunopathogenesis by type I IFN signaling-dependent impediment of Th1 cell pulmonary influx. *Nat. Commun.* **13**, 3155 (2022).
22. Sakai, S. et al. Cutting edge: control of *Mycobacterium tuberculosis* infection by a subset of lung parenchyma-homing CD4 T cells. *J. Immunol.* **192**, 2965–2969 (2014).
23. Woodworth, J. S. et al. Subunit vaccine H56/CAF01 induces a population of circulating CD4 T cells that traffic into the *Mycobacterium tuberculosis*-infected lung. *Mucosal Immunol.* **10**, 555–564 (2017).
24. Anderson, K. G. et al. Intravascular staining for discrimination of vascular and tissue leukocytes. *Nat. Protoc.* **9**, 209–222 (2014).
25. Majlessi, L., Prados-Rosales, R., Casadevall, A. & Brosch, R. Release of mycobacterial antigens. *Immunol. Rev.* **264**, 25–45 (2015).
26. Lin, P. L. et al. The multistage vaccine H56 boosts the effects of BCG to protect cynomolgus macaques against active tuberculosis and reactivation of latent *Mycobacterium tuberculosis* infection. *J. Clin. Invest.* **122**, 303–314 (2012).
27. Kwon, K. W. et al. Long-term protective efficacy with a BCG-prime ID93/GLA-SE boost regimen against the hyper-virulent *Mycobacterium tuberculosis* strain K in a mouse model. *Sci. Rep.* **9**, 15560 (2019).
28. Choi, Y. H. et al. Safety and immunogenicity of the ID93 + GLA-SE tuberculosis vaccine in BCG-vaccinated healthy adults: a randomized, double-blind, placebo-controlled phase 2 trial. *Infect. Dis. Ther.* **12**, 1605–1624 (2023).
29. Ciabattini, A. et al. Characterization of the antigen-specific CD4(+) T cell response induced by prime-boost strategies with CAF01 and CpG adjuvants administered by the intranasal and subcutaneous routes. *Front Immunol.* **6**, 430 (2015).
30. Ciabattini, A., Pettini, E. & Medaglini, D. CD4(+) T cell priming as biomarker to study immune response to preventive vaccines. *Front Immunol.* **4**, 421 (2013).
31. McAleer, J. P. & Vella, A. T. Educating CD4 T cells with vaccine adjuvants: lessons from lipopolysaccharide. *Trends Immunol.* **31**, 429–435 (2010).

32. Gyu Choi, H. et al. Importance of adjuvant selection in tuberculosis vaccine development: Exploring basic mechanisms and clinical implications. *Vaccin. X* **15**, 100400 (2023).
33. Perdomo, C. et al. Mucosal BCG vaccination induces protective lung-resident memory T cell populations against tuberculosis. *mBio* **7**, e01686–16 (2016).
34. Darrah, P. A. et al. Prevention of tuberculosis in macaques after intravenous BCG immunization. *Nature* **577**, 95–102 (2020).
35. Farinacci, M., Weber, S. & Kaufmann, S. H. The recombinant tuberculosis vaccine rBCG ΔureC::hly(+) induces apoptotic vesicles for improved priming of CD4(+) and CD8(+) T cells. *Vaccine* **30**, 7608–7614 (2012).
36. Collins, A. C. et al. Cyclic GMP-AMP synthase is an innate immune DNA sensor for *Mycobacterium tuberculosis*. *Cell Host Microbe* **17**, 820–828 (2015).
37. Moguche, A. O. et al. Antigen availability shapes T cell differentiation and function during tuberculosis. *Cell Host Microbe* **21**, 695–706.e695 (2017).
38. Clemmensen, H. S. et al. Rescuing ESAT-6 specific CD4 T cells from terminal differentiation is critical for long-term control of murine Mtb infection. *Front Immunol.* **11**, 585359 (2020).
39. Brodin, P. et al. Enhanced protection against tuberculosis by vaccination with recombinant *Mycobacterium microti* vaccine that induces T cell immunity against region of difference 1 antigens. *J. Infect. Dis.* **190**, 115–122 (2004).
40. Brodin, P. et al. Dissection of ESAT-6 system 1 of *Mycobacterium tuberculosis* and impact on immunogenicity and virulence. *Infect. Immun.* **74**, 88–98 (2006).
41. Harikumar Parvathy, G. et al. Sex differences in vaccine-induced immunity and protection against *Mycobacterium tuberculosis*. *J. Infect. Dis.* **232**, 1187–1197 (2025).
42. Jeon, B. Y. et al. *Mycobacterium bovis* BCG immunization induces protective immunity against nine different *Mycobacterium tuberculosis* strains in mice. *Infect. Immun.* **76**, 5173–5180 (2008).
43. Abebe, F. & Bjune, G. The emergence of Beijing family genotypes of *Mycobacterium tuberculosis* and low-level protection by Bacille Calmette-Guérin (BCG) vaccines: is there a link? *Clin. Exp. Immunol.* **145**, 389–397 (2006).
44. Whittaker, E. et al. Age-related waning of immune responses to BCG in healthy children supports the need for a booster dose of BCG in TB endemic countries. *Sci. Rep.* **8**, 15309 (2018).
45. Kwon, K. W. et al. BCGΔBCG1419c increased memory CD8(+) T cell-associated immunogenicity and mitigated pulmonary inflammation compared with BCG in a model of chronic tuberculosis. *Sci. Rep.* **12**, 15824 (2022).
46. Kwon, K. W. et al. *Mycobacterium tuberculosis*-specific T cells restrain anti-cancer drug-induced neutrophilic lung inflammation in tuberculosis. *Nat. Commun.* **16**, 8875 (2025).
47. Choi, E. et al. Permissive lung neutrophils facilitate tuberculosis immunopathogenesis in male phagocyte NADPH oxidase-deficient mice. *PLoS Pathog.* **20**, e1012500 (2024).

Acknowledgements

This work was supported by the National Research Foundation of Korea (NRF) grant funded by the Ministry of Science and Information and Communication Technology (MSIT) (RS-2023-00208115), by the Korea Health Technology R&D Project through the Korea Health Industry Development Institute (KHIDI) funded by the Ministry of Health & Welfare, Republic of Korea (RS-2025-02173063), and by a grant from the Ministry of Food and Drug Safety (26202MFDS013) in 2026, Republic of Korea. We acknowledge the NIH Tetramer Core Facility for provision of I-A(b):ESAT-$6_{4\text{-}17}$ and corresponding negative control tetramers I-A(b):hCLIP.

Author contributions

Conceptualization: R.B. and S.J.S.; Funding acquisition: S.J.S.; Investigation: K.W.K. and Hongmin Kim; Methodology: K.W.K., Hongmin Kim, and Hagyu Kim; Supervision: R.B. and S.J.S.; Validation: R.B. and S.J.S.; Writing-original draft: K.W.K., Hongmin Kim, R.B. and S.J.S.; Writing-review and editing: K.W.K., Hongmin Kim, R.B. and S.J.S. with inputs from all authors.; K.W.K. and Hongmin Kim are co-first authors of this manuscript.

Competing interests

The authors declare no competing interests.

Additional information

Supplementary information The online version contains supplementary material available at https://doi.org/10.1038/s41541-026-01439-3.

Correspondence and requests for materials should be addressed to Roland Brosch or Sung Jae Shin.